

Supporting information

of

**N-(2-(Diphenylphosphino)ethyl)-2-alkyl-5,6,7,8-tetrahydroquinolin-8-amines
iron(II) complexes: Structural diversity and the ring opening polymerization of
ε-caprolactone**

Yun Wang,^{a,b,c} Wenjuan Zhang,^{*,a,b} Xing Wang,^{b,c} Weiwei Zuo,^{*,a} Xiaopan Xue,^b
Yanping Ma,^a Wen-Hua Sun^{*,c}

Table of contents

Page

1. Fig. S1 ^1H NMR spectrum of L5	S2
2. Fig. S2 ^{13}C NMR spectrum of L5	S2
3. Fig. S3 ^{31}P NMR spectrum of L5	S3
4. Fig. S4 ^1H NMR spectrum of L6	S3
5. Fig. S5 ^{13}C NMR spectrum of L6	S4
6. Fig. S6 ^{31}P NMR spectrum of L6	S4
7. Fig. S7 ^1H NMR spectrum of L7	S5
8. Fig. S8 ^{13}C NMR spectrum of L7	S5
9. Fig. S9 The monitoring ^{31}P NMR spectrum of L4 in CDCl_3	S6
10. Fig. S10 The monitoring ^{31}P NMR spectrum of L1 in CDCl_3	S6
11. Fig. S11 MALDI-TOF mass spectrum of the PCL obtained using Fe6 ($[\varepsilon\text{-CL}]/[\text{Fe}] = 100:1$, $T = 30^\circ\text{C}$, $t = 10 \text{ min}$)	S7
12. Fig. S12 ^1H NMR spectrum of the PCL obtained using Fe6 ($[\varepsilon\text{-CL}]/[\text{Fe}] = 100:1$, $T = 30^\circ\text{C}$, $t = 10 \text{ min}$)	S7
13. Fig. S13 MALDI-TOF mass spectrum of the PCL obtained using Fe6 ($[\varepsilon\text{-CL}]/[\text{Fe}] = 400:1$, $T = 30^\circ\text{C}$, $t = 10 \text{ min}$)	S8
14. Fig. S14 ^1H NMR spectrum of the PCL obtained using Fe6 ($[\varepsilon\text{-CL}]/[\text{Fe}] = 400:1$, $T = 30^\circ\text{C}$, $t = 10 \text{ min}$)	S8
15. Fig. S15 MALDI-TOF mass spectrum of the PCL obtained using Fe6 ($[\varepsilon\text{-CL}]/[\text{Fe}] = 800:1$, $T = 30^\circ\text{C}$, $t = 10 \text{ min}$)	S9
16. Fig. S16 ^1H NMR spectrum of the PCL obtained using Fe6 ($[\varepsilon\text{-CL}]/[\text{Fe}] = 800:1$, $T = 30^\circ\text{C}$, $t = 10 \text{ min}$)	S9
17. Table S1 Crystal data and structure refinements for Fe4'	S10
18. Table S2 Selected bond lengths (\AA) and angles ($^\circ$) for Fe4'	S10
19. Fig. S17 The GPC spectra of high molecular PCL using Fe6 ($[\varepsilon\text{-CL}]/[\text{Fe}] = 1800:1$, $T = 90^\circ\text{C}$, $t = 10 \text{ min}$)	S11
20. Fig. S18 The GPC spectra of high molecular PCL using Fe6 ($[\varepsilon\text{-CL}]/[\text{Fe}] = 2000:1$, $T = 90^\circ\text{C}$, $t = 10 \text{ min}$)	S11
21. Fig. S19 The GPC spectra of high molecular PCL using Fe4 ($[\varepsilon\text{-CL}]/[\text{Fe}] = 1500:1$, $T = 90^\circ\text{C}$, $t = 10 \text{ min}$)	S12
22. Fig. S20 The GPC spectra of high molecular PCL using Fe5 ($[\varepsilon\text{-CL}]/[\text{Fe}] = 1500:1$, $T = 90^\circ\text{C}$, $t = 10 \text{ min}$)	S12
23. Fig. S21 ^1H NMR spectrum of L8	S13

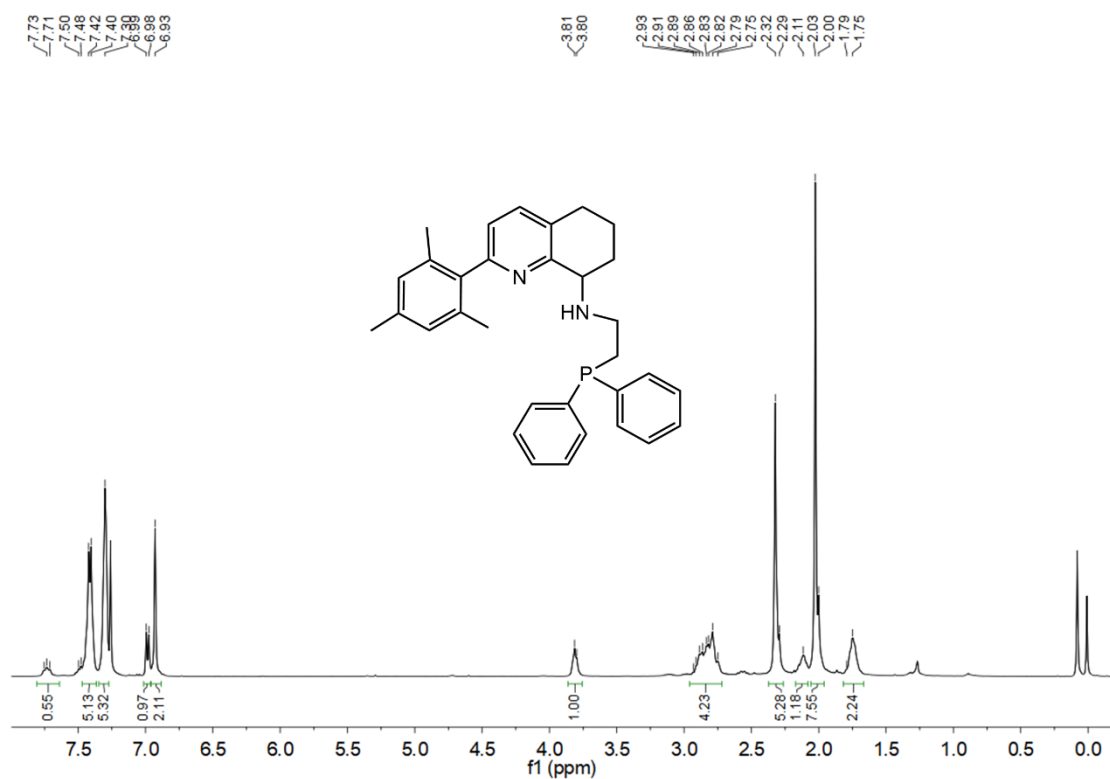


Fig. S1 ^1H NMR (CDCl_3 , 25°C) spectrum of L5

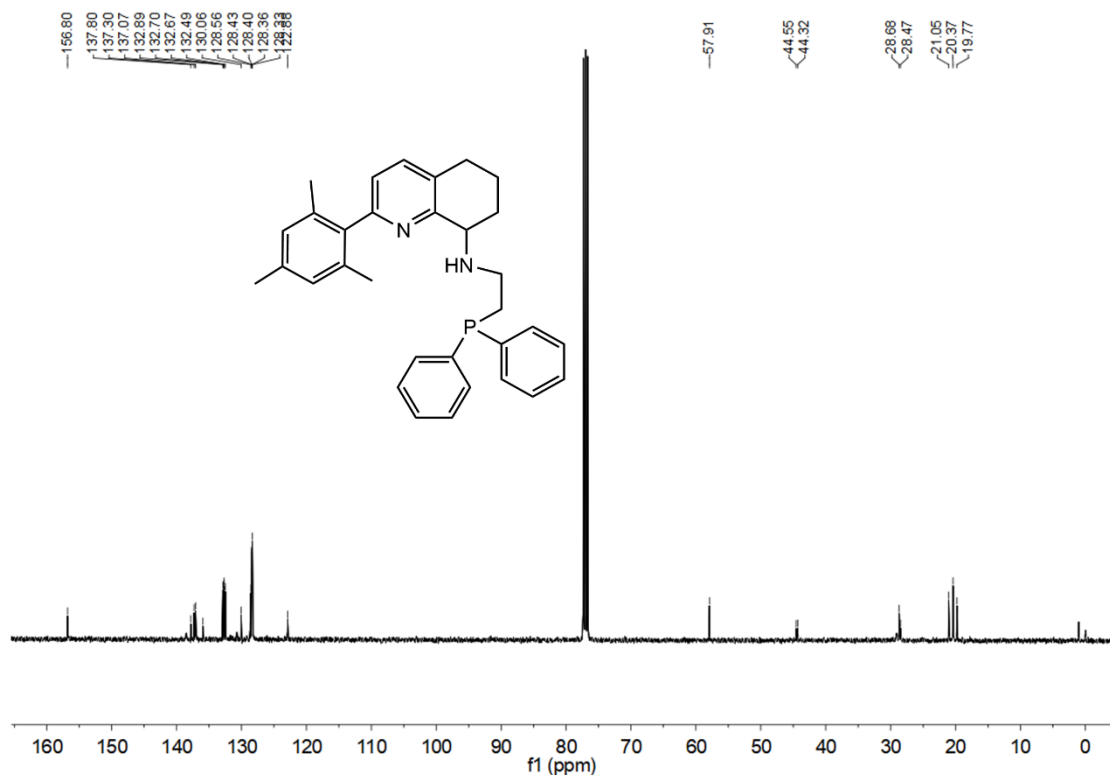


Fig. S2 ^{13}C NMR (CDCl_3 , 25°C) spectrum of L5

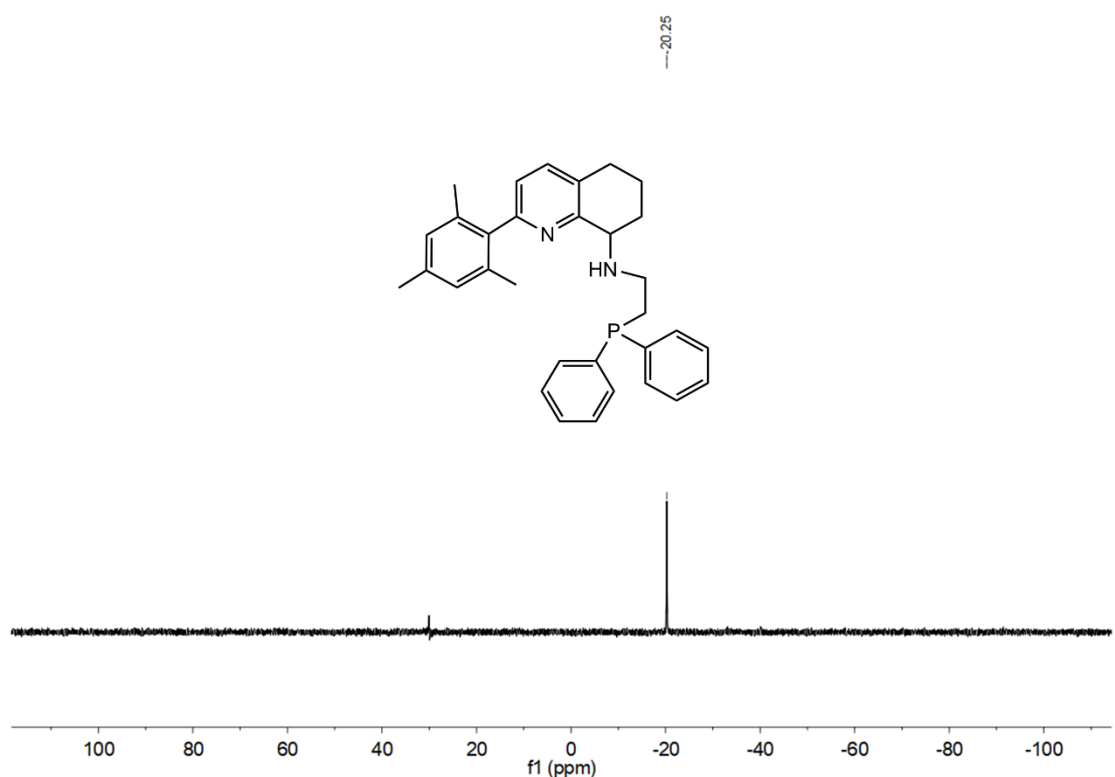


Fig. S3 ^{31}P NMR (CDCl_3 , 25°C) spectrum of **L5**

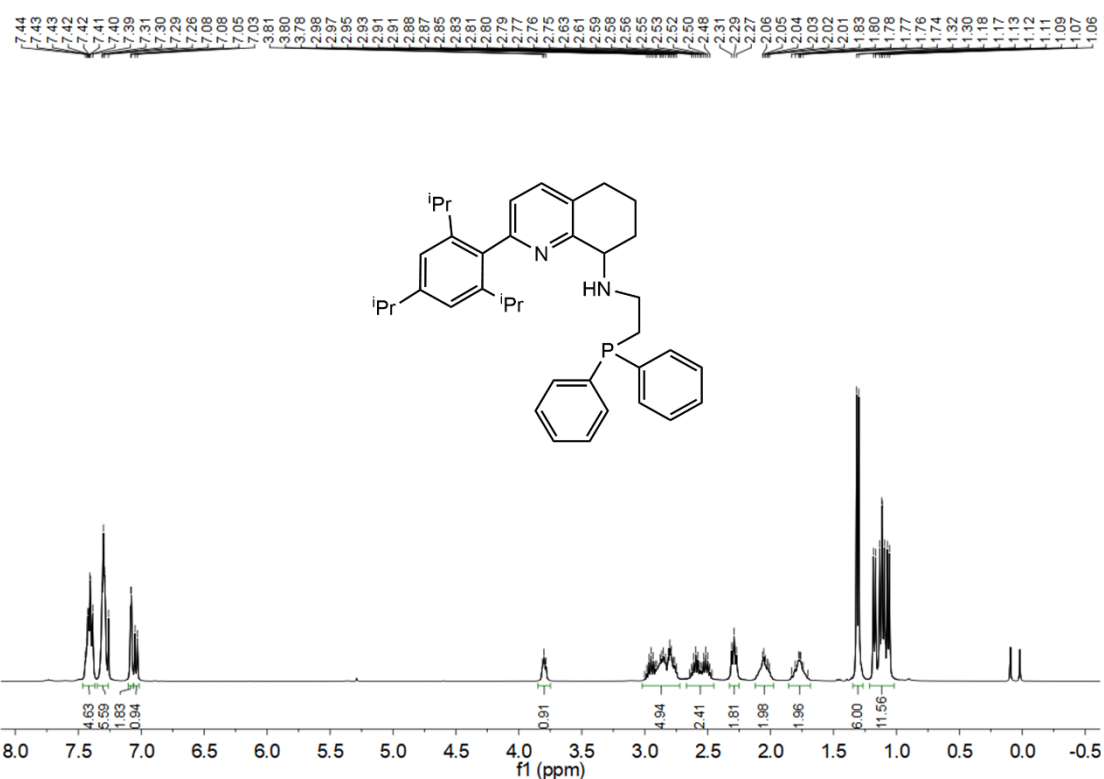


Fig. S4 ^1H NMR (CDCl_3 , 25°C) spectrum of **L6**

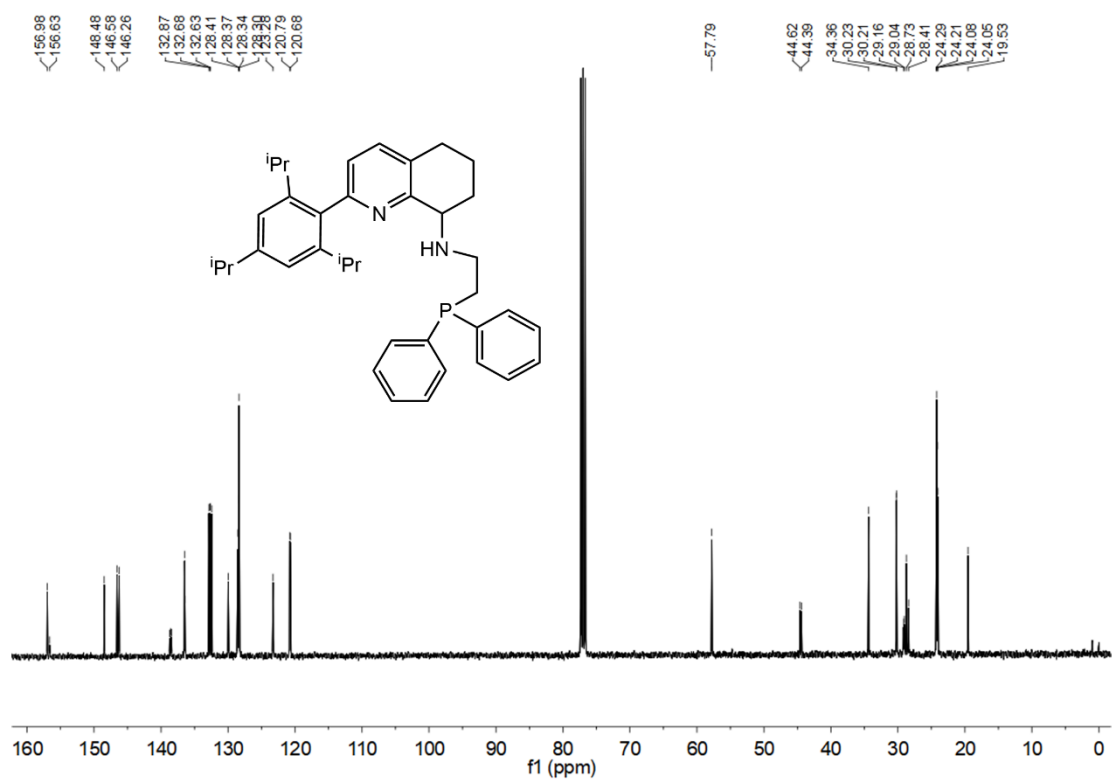


Fig. S5 ^{13}C NMR (CDCl_3 , 25°C) spectrum of **L6**

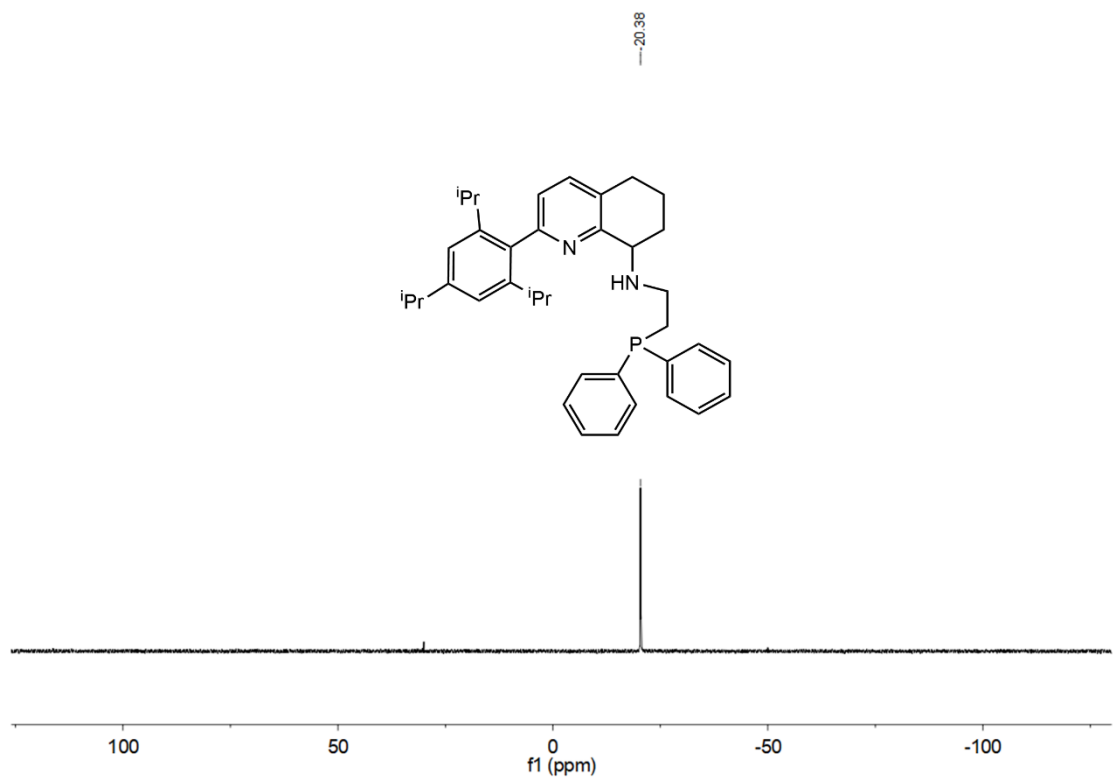


Fig. S6 ^{31}P NMR (CDCl_3 , 25°C) spectrum of **L6**

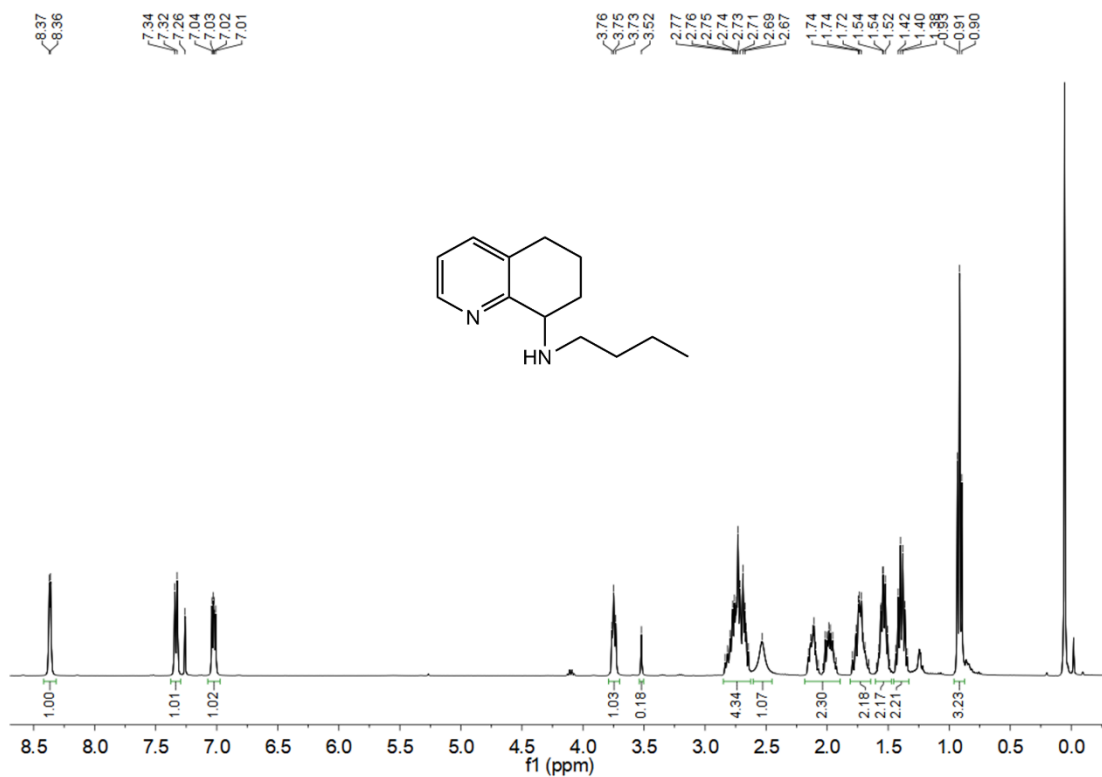


Fig. S7 ^1H NMR (CDCl_3 , 25°C) spectrum of **L7**

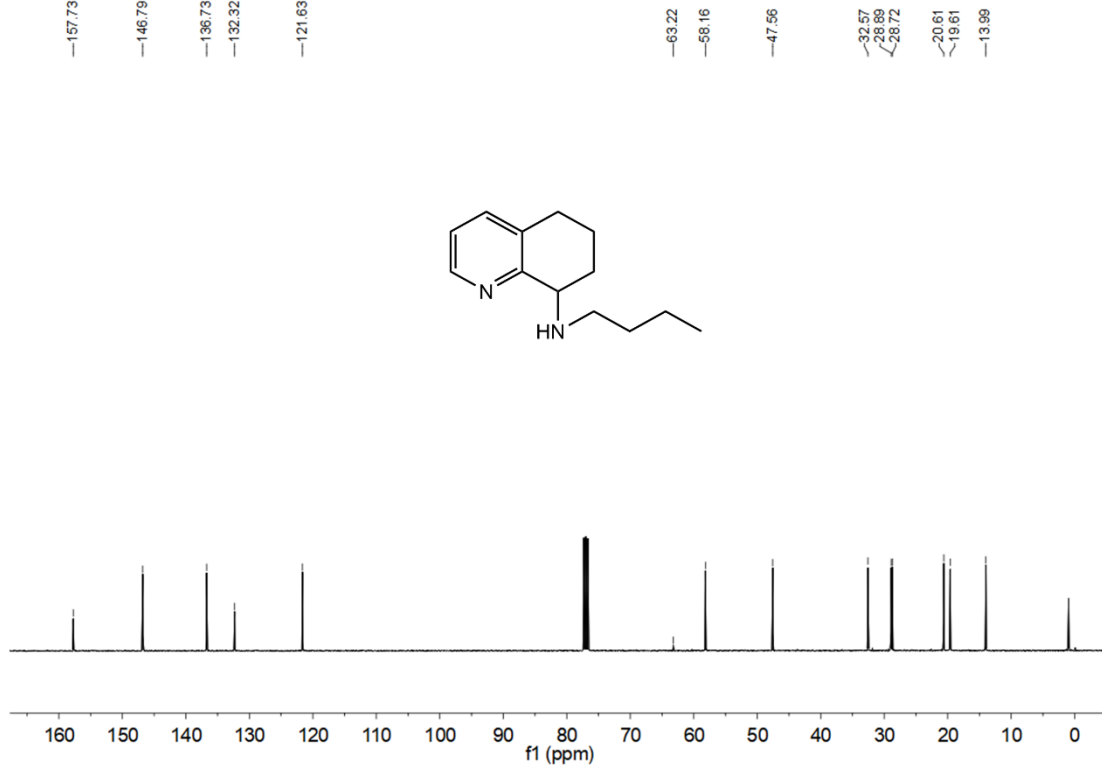


Fig. S8 ^{13}C NMR (CDCl_3 , 25°C) spectrum of L7

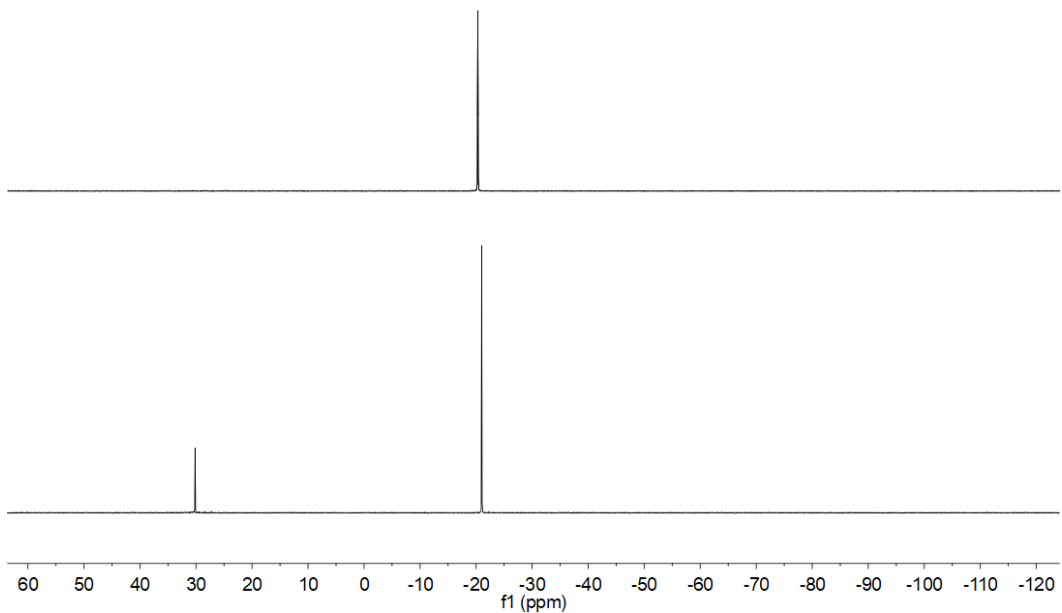


Fig. S9 The monitoring ^{31}P NMR spectra of **L4** in CDCl_3 (top) and **L4** in CDCl_3 (bottom, two weeks later)

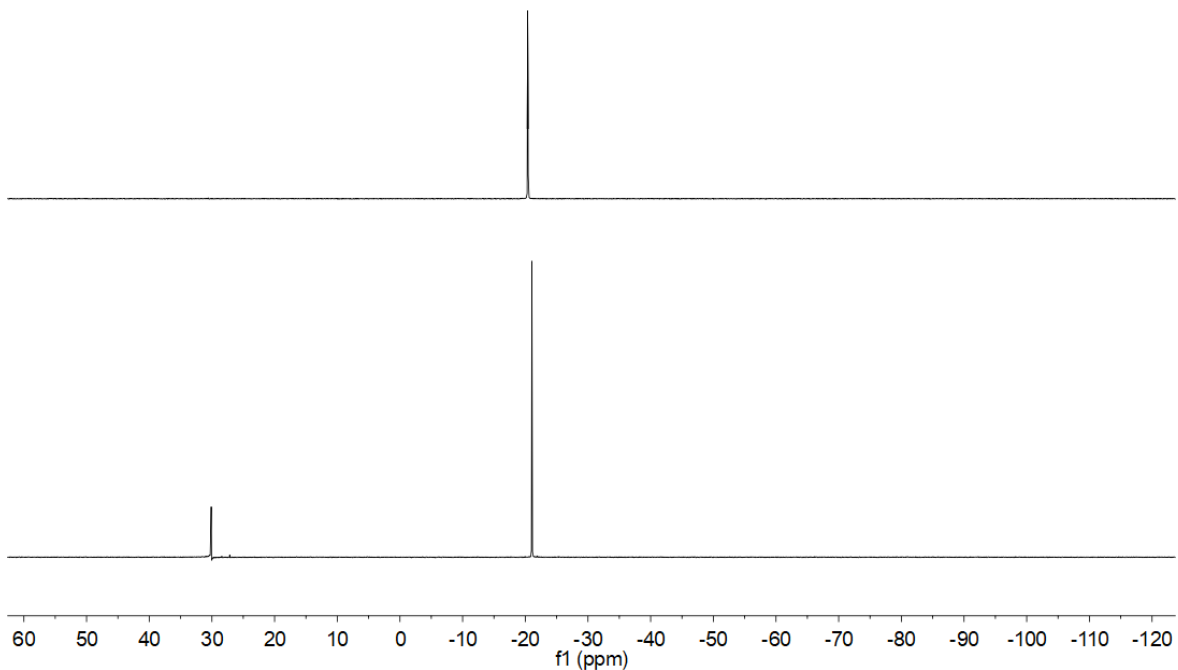


Fig. S10 The monitoring ^{31}P NMR spectra of **L1** in CDCl_3 (top) and **L1** in CDCl_3 (bottom, two weeks later)

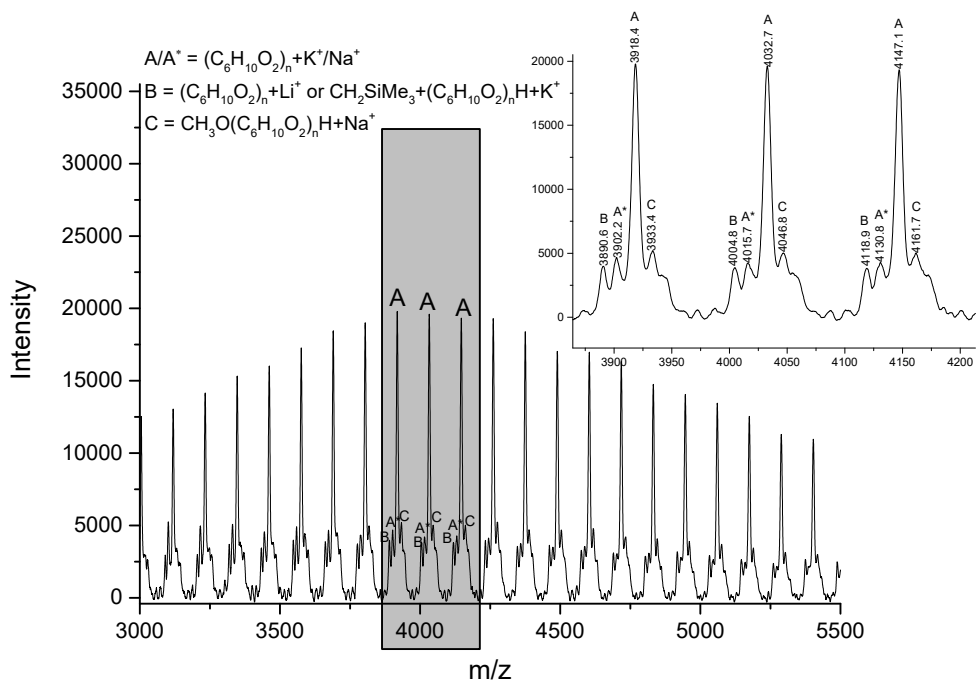


Fig. S11 MALDI-TOF mass spectrum of the PCL obtained using **Fe6** ($[\varepsilon\text{-CL}]/[\text{Fe}] = 100:1$, $T = 30^\circ\text{C}$, $t = 10 \text{ min}$)

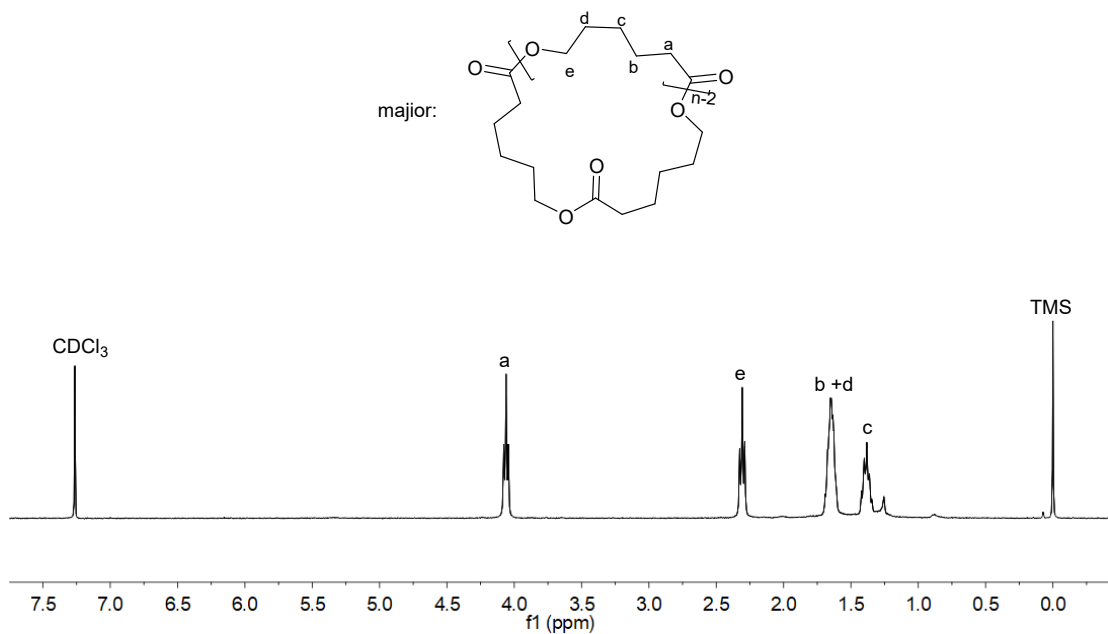


Fig. S12 ^1H NMR spectrum of the PCL obtained using **Fe6** ($[\varepsilon\text{-CL}]/[\text{Fe}] = 100:1$, $T = 30^\circ\text{C}$, $t = 10 \text{ min}$)

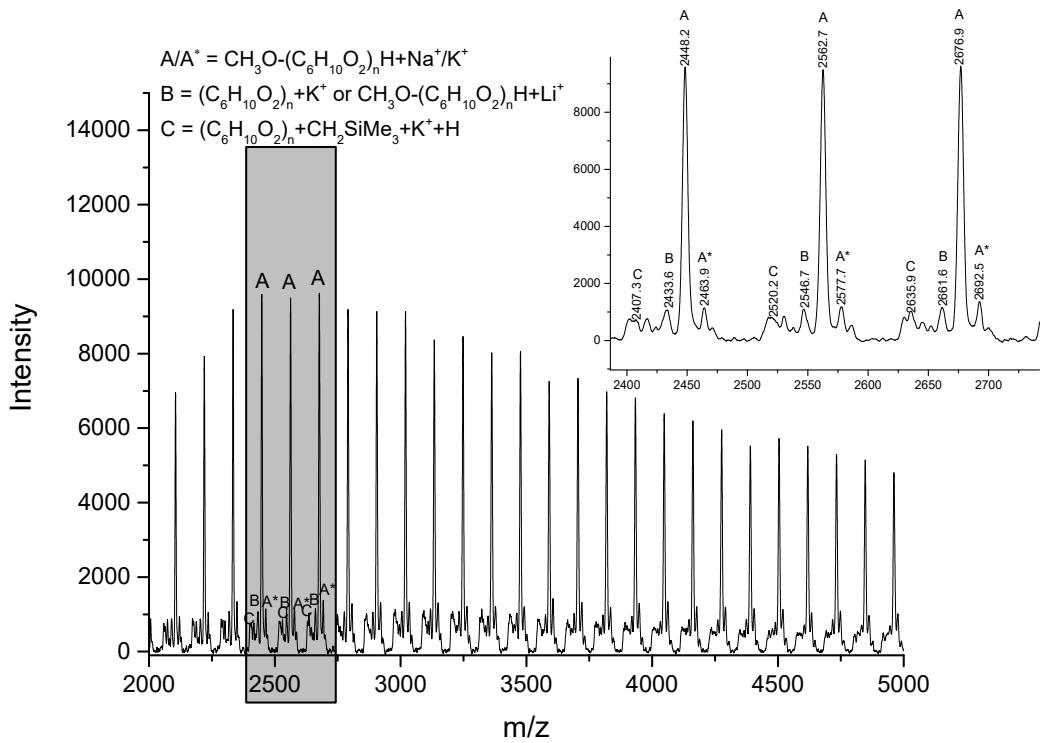


Fig. S13 MALDI-TOF mass spectrum of the PCL obtained using **Fe6** ($[\varepsilon\text{-CL}]/[\text{Fe}] = 400:1$, $T = 30^\circ\text{C}$, $t = 10\text{ min}$)

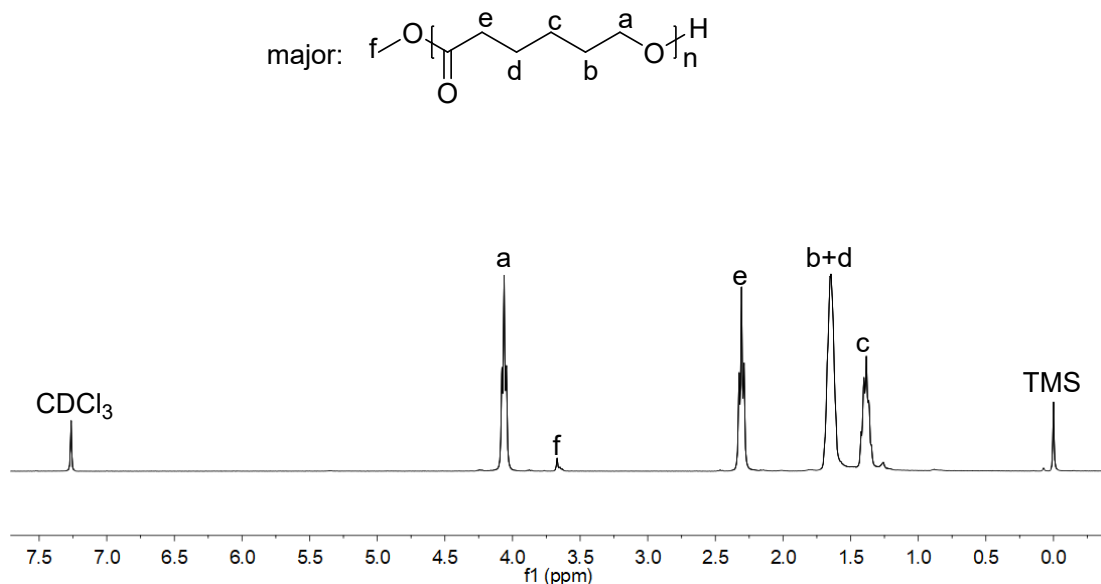


Fig. S14 ^1H NMR spectrum of the PCL obtained using **Fe6** ($[\varepsilon\text{-CL}]/[\text{Fe}] = 400:1$, $T = 30^\circ\text{C}$, $t = 10 \text{ min}$)

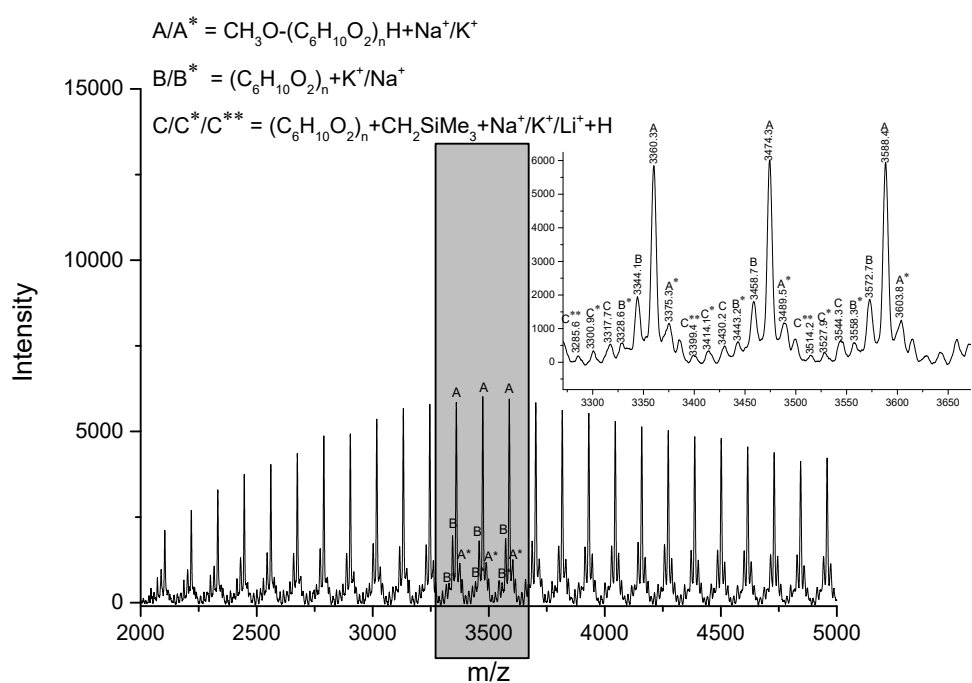


Fig. S15 MALDI-TOF mass spectrum of the PCL obtained using **Fe6** ($[\varepsilon\text{-CL}]/[\text{Fe}] = 800:1$, $T = 30^\circ\text{C}$, $t = 10 \text{ min}$)

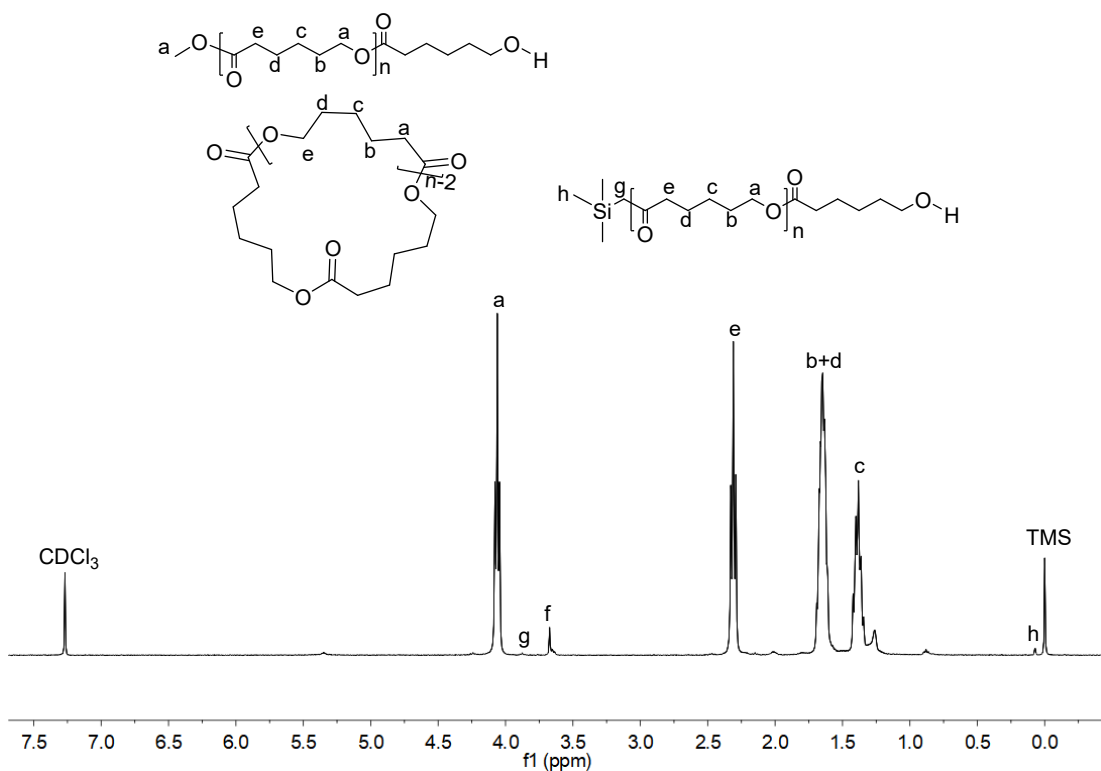


Fig. S16 ¹H NMR spectrum of the PCL obtained using **Fe6** ($[\varepsilon\text{-CL}]/[\text{Fe}] = 800:1$, $T = 30^\circ\text{C}$, $t = 10 \text{ min}$)

Table S1 Crystal data and structure refinements for **Fe4'**

Fe4'	
empirical formula	$\text{C}_{23}\text{H}_{24}\text{Cl}_5\text{Fe}_{1.5}\text{N}_2\text{OP}$
formula weight	636.44
temperature/K	169.98(10)
crystal system	monoclinic
space group	$\text{P}2_1/\text{n}$
$a/\text{\AA}$	12.0592(3)
$b/\text{\AA}$	15.9546(4)
$c/\text{\AA}$	13.9879(3)
$\alpha/^\circ$	90
$\beta/^\circ$	94.627(2)
$\gamma/^\circ$	90
volume/ \AA^3	2682.50(11)
Z	4
$\rho_{\text{calc}}/\text{g cm}^{-3}$	1.576
μ/mm^{-1}	11.901
$F(000)$	1292.0
crystal size/ mm^3	$0.2 \times 0.12 \times 0.1$
radiation	$\text{CuK}\alpha (\lambda = 1.54184)$

2θ range for data collection/°	8.422 to 154.838
index ranges	-15 ≤ h ≤ 14, -19 ≤ k ≤ 20, -17 ≤ l ≤ 16
reflections collected	22038
independent reflections	5463 [R _{int} = 0.0738, R _{sigma} = 0.0545]
data/restraints/parameters	5463/0/304
goodness-of-fit on F ²	1.043
final R indices [I>=2σ (I)]	R ₁ = 0.0537, wR ₂ = 0.1424
final R indices [all data]	R ₁ = 0.0636, wR ₂ = 0.1502
largest diff. peak/hole/ e Å ⁻³	0.97/-0.67

Table S2 Selected bond lengths (Å) and angles (°) **Fe4'**

Bond length (Å)			
Fe1-N1	2.287(3)	P1-O1	1.501(2)
Fe1-N2	2.251(3)	N2-C8	1.479(4)
Fe1-O1	2.046(2)		
Bond angles (°)			
O1-Fe1-N1	91.68(9)	O1-P1-C11	111.20(14)
O1-Fe1-N2	91.37(9)	C8-N2-Fe1	106.34(18)
N2-Fe1-N1	73.44(9)	P1-O1-Fe1	127.93(13)

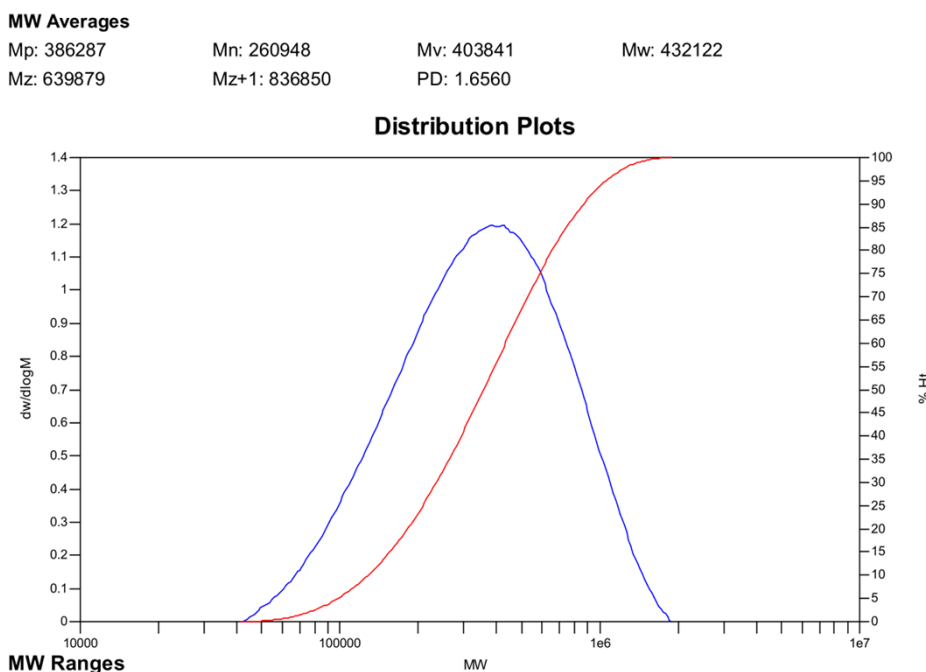


Fig. S17 The GPC spectra of high molecular PCL using **Fe6** ([ε-CL]/[Fe] = 1800:1, T = 90 °C, t = 10 min)

MW AveragesMp: 386287
Mz: 672520Mn: 239393
Mz+1: 879051Mv: 411039
PD: 1.8506

Mw: 443009

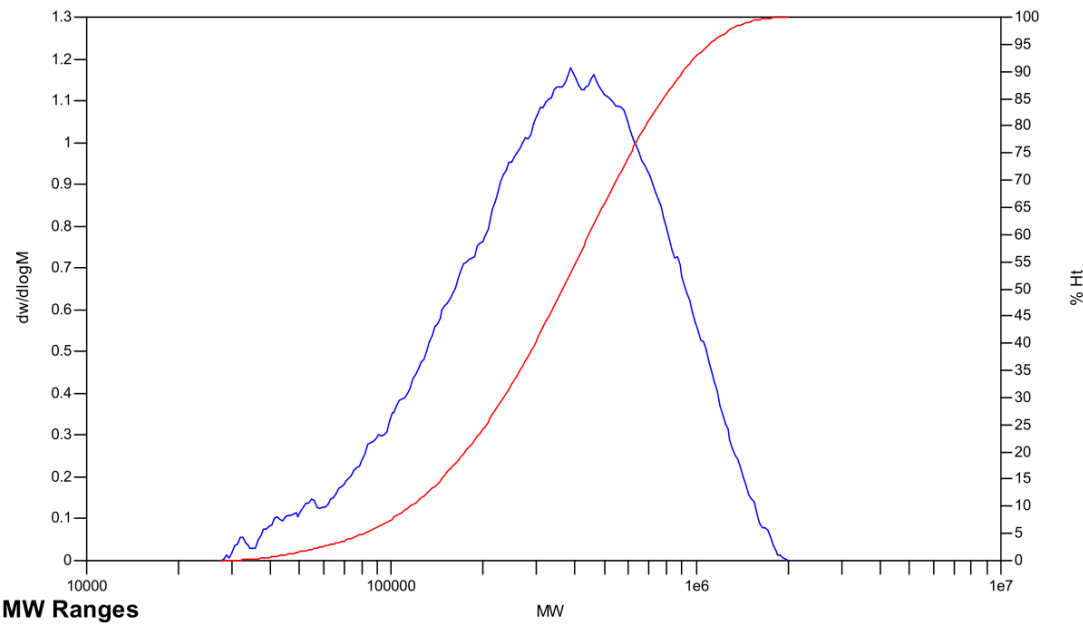
Distribution Plots

Fig. S18 The GPC spectra of high molecular PCL using **Fe6** ($[\epsilon\text{-CL}]/[\text{Fe}] = 2000:1$, T = 90 °C, t = 10 min)

MW AveragesMp: 418688
Mz: 865541Mn: 219258
Mz+1: 1227595Mv: 449554
PD: 2.2666

Mw: 496962

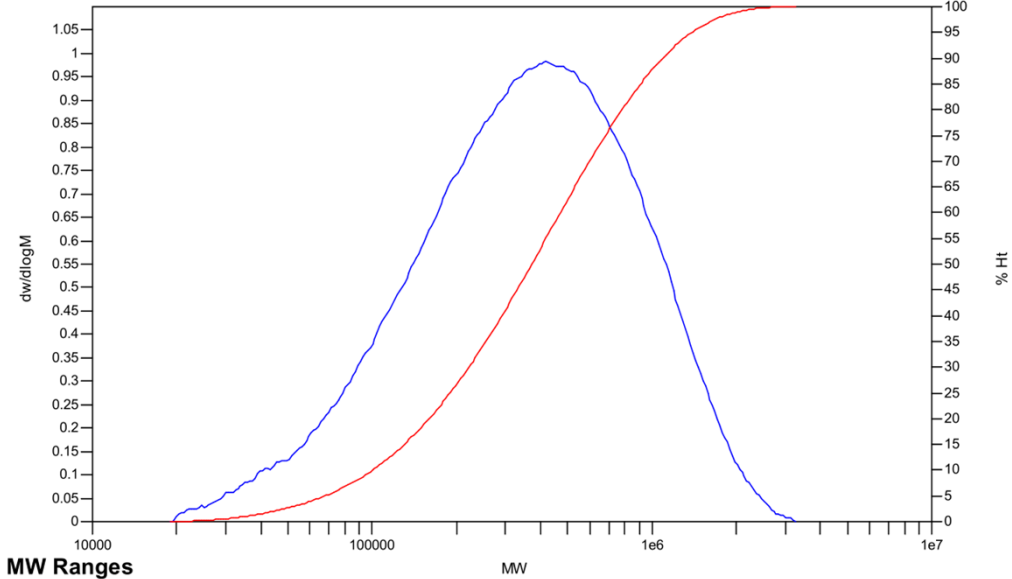
Distribution Plots

Fig. S19 The GPC spectra of high molecular PCL using **Fe4** ($[\epsilon\text{-CL}]/[\text{Fe}] = 1500:1$, T = 90 °C, t = 10 min)

MW AveragesMp: 386287
Mz: 688598Mn: 243463
Mz+1: 901882Mv: 416567
PD: 1.8469

Mw: 449661

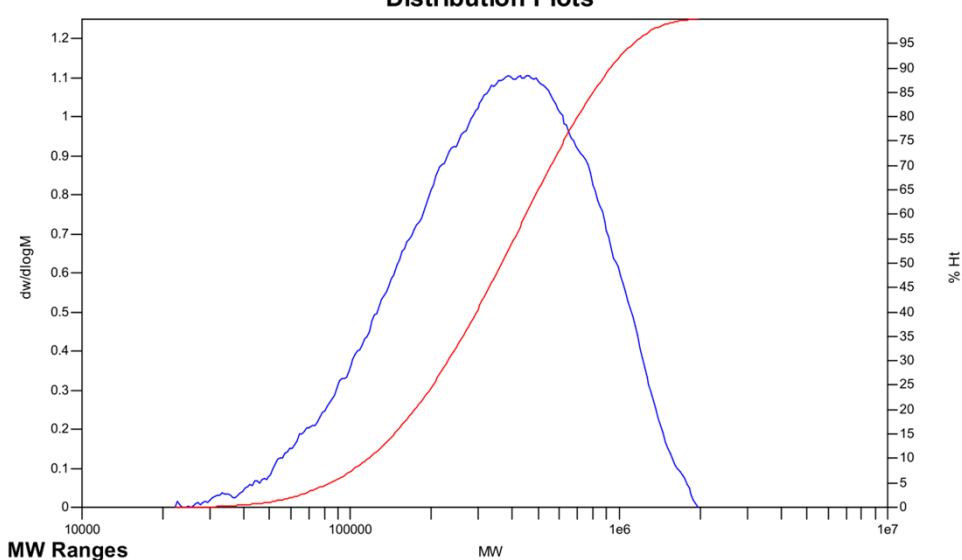
Distribution Plots

Fig. S20 The GPC spectra of high molecular PCL using **Fe5** ($\text{[}\varepsilon\text{-CL]}/[\text{Fe}] = 1500:1$, T = 90 °C, t = 10 min)

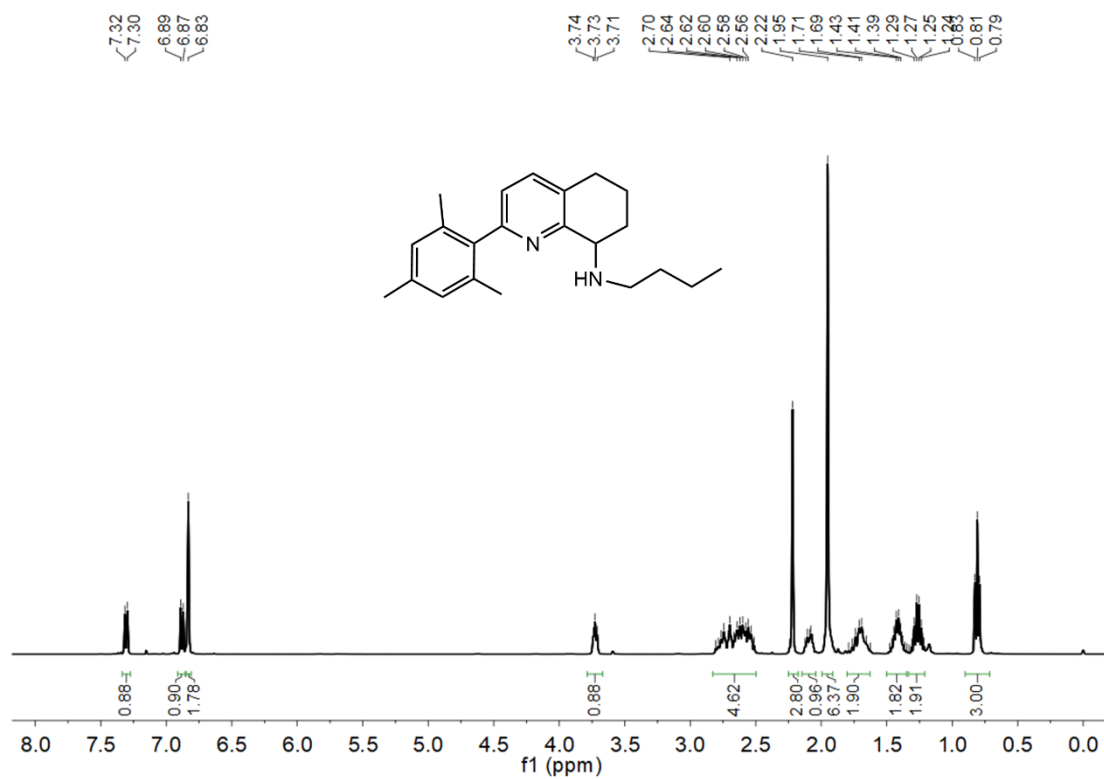


Fig. S21 ^{13}C NMR (CDCl_3 , 25 °C) spectrum of **L8**